

GEO-R1: IMPROVING FEW-SHOT GEOSPATIAL REFERRING EXPRESSION UNDERSTANDING WITH REINFORCEMENT FINE-TUNING

Zilun Zhang, Zian Guan*, Tiancheng Zhao, Haozhan Shen, Tianyu Li, Yuxiang Cai, Zhonggen Su, & Jianwei Yin
 Zhejiang University
 {zilun.zhang, guanbian}@zju.edu.cn
 tianchez@zju-bj.com

Zhaojun Liu
 China Academy of Space Technology
 bisme@china.com

Xiang Li
 University of Bristol
 xiang92.li@bristol.ac.uk

ABSTRACT

Referring expression understanding in remote sensing poses unique challenges, as it requires reasoning over complex object–context relationships. While supervised fine-tuning (SFT) on multimodal large language models achieves strong performance with massive labeled datasets, they struggle in data-scarce scenarios, leading to poor generalization. To address this limitation, we propose Geo-R1, a reasoning-centric reinforcement fine-tuning (RFT) paradigm for few-shot geospatial referring. Geo-R1 enforces the model to first generate explicit, interpretable reasoning chains that decompose referring expressions, and then leverage these rationales to localize target objects. This “reason first, then act” process enables the model to make more effective use of limited annotations, enhances generalization, and provides interpretability. We validate Geo-R1 on three carefully designed few-shot geospatial referring benchmarks, where our model consistently and substantially outperforms SFT baselines. It also demonstrates strong cross-dataset generalization, highlighting its robustness. Code and data will be released at <http://geo-r1.github.io>.

1 INTRODUCTION

Vision language models (VLMs) have become a critical tool for remote sensing imagery (RSI) understanding (Li et al., 2024c; Weng et al., 2025). By coupling natural language with RSI, VLMs can drive a wide spectrum of tasks in the RS domain, such as image captioning, visual question answering, referring expression comprehension (REC), referring expression segmentation (RES) (Li et al., 2024c; Zhou et al., 2024a). Among these capabilities, REC and RES tasks are especially important: both require the model to resolve free-form linguistic descriptions (e.g., “a small vehicle is situated at the bottom right adjacent to a large vehicle”) into concrete, spatially localized predictions (bounding boxes or segmentation masks) in high-resolution aerial images. We henceforth use the term *Referring Expression Understanding* (REU) to denote a unified framework encompassing both REC and RES, where the task is to take an image and a text query as input and output one or more target objects.

Although recent works (Kuckreja et al., 2024; Yuan et al., 2024; Zhou et al., 2024b) have achieved remarkable progress on REU tasks with supervised finetuning (SFT), these methods are highly dependent on large-scale training labels. High-quality REU supervision demands not only image-level labels but also precise language–region alignment at the object and region levels. Creating such associations in overhead imagery requires expertise and careful tooling: annotators must parse complex scene layouts, disambiguate visually similar man-made structures, and write unambiguous referring expressions before drawing spatially accurate boxes or masks. Compared with image-level

*Zilun Zhang and Zian Guan contributed equally

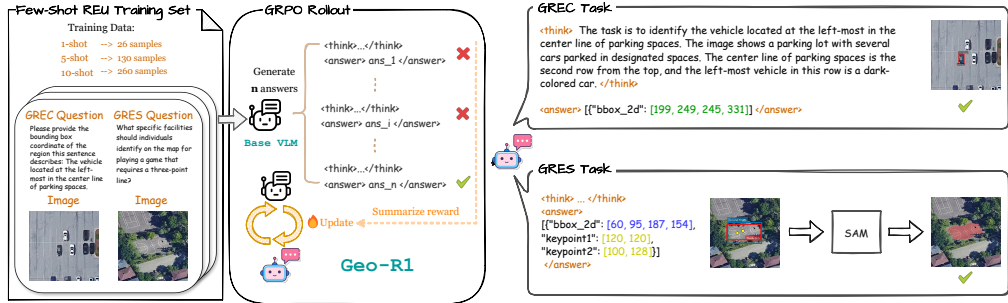


Figure 1: Geo-R1 method overview. Geo-R1 is trained on a few labeled samples with reinforcement learning (e.g., GRPO (Shao et al., 2024)) and can identify target objects (bounding boxes or masks) from an input image and text query while providing the reasoning process.

labels, these fine-grained annotations are orders of magnitude more labor-intensive. For example, VRSBench (Li et al., 2024b) costs 1,004 labor hours for label verification only.

This reality makes few-shot learning (e.g., only 10 samples are provided for each category) in REU valuable. Previous works, such as RS-CLIP(Li et al., 2023) and RemoteCLIP (Liu et al., 2024a) have demonstrated that finetuning CLIP (Radford et al., 2021) on a few samples can yield strong results for scene classification. However, these advances cannot be directly carried over to REU since region-level grounding is harder than scene-level classification. Moreover, object relations are complex for REU, requiring relational reasoning and disambiguation among visually similar structures. This raises the question: *with only a handful of aligned examples for each category, can a VLM learn to accurately ground language in remote sensing images?*

Driven by the impressive reasoning capabilities of OpenAI o1 (Jaech et al., 2024) and DeepSeek-R1 (Guo et al., 2025), reinforcement learning (RL) has become a powerful post-training paradigm for augmenting the reasoning capabilities of LLMs during post-training. RL explicitly encourages intermediate “thinking” steps, and forces the model learns to reason before committing to a prediction. This reasoning-first behavior is particularly well suited to few-shot REU: reasoning steps (e.g., “My intuition leads me to identify the vehicle sitting in the circular opening near the roadway as the small vehicle.”) serve as a transferable experience that generalizes better across different text-image samples than directly outputting a box/mask from next-token-prediction supervision.

In this work, we introduce a reasoning-centric RL post-training method, Geo-R1, which leverages task-specific reward functions to address few-shot REU. Geo-R1 encourages the model to generate explicit reasoning—intermediate hypotheses that parse the referring expression, identify contextual anchors, and iteratively refine localization—thereby regularizing learning and improving generalization. Unlike SFT, which relies on a single teacher-forced trajectory with a differentiable surrogate loss, Geo-R1 explores multiple reasoning chains and proposals, extracting advantages from N -way comparisons to provide denser and richer supervision per example, making better use of few-shot samples. Moreover, for RES, Geo-R1 directly optimizes a task-aligned $MaskIoU$ reward through the non-differentiable “BBox + SAM” pipeline (Ravi et al., 2025), enabling end-to-end training for dense prediction—a capability infeasible under SFT. Method overview can be found in Fig. 1.

In our experiments, we observe three consistent advantages from RL over SFT baselines for few-shot REU in remote sensing images. (1) With the same small number of labeled examples, our RFT-based reasoning model substantially outperforms SFT-based models on few-shot REU tasks. (2) In cross-dataset evaluation, our RFT-based model remarkably outperforms SFT counterparts, suggesting the reasoning model has stronger cross-dataset generalization than non-reasoning models. (3) The learned reasoning traces are concise and reasonable, utilizing the spatial and semantic cues that benefit the final localization, which provides a great interpretability. We further establish three few-shot benchmarks and define a few-shot protocol for REU. In summary, our contributions are listed below:

- To the best of our knowledge, we are the first to explore Referring Expression Understanding (REU) for aerial image understanding under few-shot settings. To facilitate rigorous and reproducible evaluation, we create VRSBench-FS, EarthReason-FS, and NWPU-FS, establishing standardized protocols for few-shot REU in remote sensing.

- We define task-aligned rewards and a reasoning-centric RL recipe, including BBoxIoU reward for REC and a MaskGIoU reward for RES. We introduce the RL-trained reasoning models (Geo-R1) that generate concise grounding rationales for these tasks.
- Across all three benchmarks, our Geo-R1 models consistently outperform SFT under identical few-shot budgets, while exhibiting stronger generalization across datasets and providing human-auditable reasoning traces that explain successes and failures.

2 TASK AND METHODOLOGY

This section details the adaptation of the GRPO algorithm from language-only tasks to vision-language tasks. Then, we introduce and formally define the REU task under few-shot settings. Finally, we discuss how to apply GRPO to these tasks with customized task-specific reward functions.

2.1 GRPO: FROM LLM TO VLM

Building upon the foundation of reinforcement learning algorithms like Proximal Policy Optimization (PPO) (Schulman et al., 2017), Group Relative Policy Optimization (GRPO) (Shao et al., 2024) has become a more effective and memory-efficient evolution for training advanced reasoning models by eliminating the value model and changing the reward model to rule-based reward. The advantage is estimated in a group-relative manner, simplifying the training process.

The GRPO algorithm begins by sampling N candidate outputs $\{o_1, \dots, o_N\}$ from the current policy π_θ for a given query prompt q . Each response o_i is then evaluated by a reward function $R(q, o_i)$ to obtain a raw reward score r_i . To measure the relative quality of each response within the sampled group, GRPO standardizes the raw rewards to obtain the advantage value, as shown in Eq. 1. The advantage value \hat{A}_i denotes the normalized advantage of the response o_i relative to other samples within the group.

$$\hat{A}_i = \frac{r_i - \text{mean}\{r_1, r_2, \dots, r_N\}}{\text{std}\{r_1, r_2, \dots, r_N\}} \quad (1)$$

The policy π_θ is updated with a training objective (Eq. 2), designed to encourage the generation of responses with higher advantages.

$$\mathcal{J}_{\text{GRPO}}(\theta) = \mathbb{E}_{\{o_i\}_{i=1}^N \sim \pi_{\theta_{\text{old}}}(\cdot|q)} \left[\frac{1}{N} \sum_{i=1}^N \left(\min(c_1 \cdot \hat{A}_i, c_2 \cdot \hat{A}_i) - \beta D_{\text{KL}}(\pi_\theta || \pi_{\text{ref}}) \right) \right], \quad (2)$$

where

$$c_1 = \frac{\pi_\theta(o_i | q)}{\pi_{\theta_{\text{old}}}(o_i | q)}, c_2 = \text{clip}\left(\frac{\pi_\theta(o_i | q)}{\pi_{\theta_{\text{old}}}(o_i | q)}, 1 - \varepsilon, 1 + \varepsilon\right). \quad (3)$$

Here, $D_{\text{KL}}(\pi_\theta || \pi_{\text{ref}})$ denotes the KL divergence between the current policy π_θ and the reference policy π_{ref} , which serves as a regularization term to prevent large deviations. The clipping mechanism in c_2 stabilizes training by constraining the policy update ratio.

For LLMs on tasks with definitive answers, like mathematical reasoning, this reward can be calculated using a rule-based verifiable reward function. By applying a reward to the thinking process and using the GRPO algorithm, DeepSeek-R1 (Guo et al., 2025) can provide both final answers and the logical reasoning process that leads to them. This approach can be extended to VLMs by converting visual metrics into tailored reward signals. Recently, there are some works that adapt GRPO for vision-language tasks by engineering task-specific rewards, such as VLM-R1 (Shen et al., 2025), Visual-RFT (Liu et al., 2025b), Seg-Zero (Liu et al., 2025a), etc.

2.2 FEW-SHOT REFERRING EXPRESSION UNDERSTANDING TASK

Referring Expression Understanding (REU) serves as a unifying framework for Generalized Referring Expression Comprehension (GREC) and Generalized Referring Expression Segmentation (GRES). Given an image I and a textual query q , a vision-language model (VLM) \mathcal{F} predicts one or more target objects, as formulated in Eq. 4:

$$\{O_1, \dots, O_N\} = \mathcal{F}(I, q), \quad (4)$$

where each O_i denotes a predicted object parsed from VLM text outputs, and N denotes the number of parsed objects. In the case of GREC, O_i is represented as a bounding box, while for GRES, O_i is represented as an instance mask.

Tasks such as REC, RES, Generalized REC (GREC) (He et al., 2023), Generalized RES (GRES) (Liu et al., 2023), Visual Grounding (VG) (Plummer et al., 2015), Open-Vocabulary Detection (OVD), and Open-Vocabulary Segmentation (OVS) (Wu et al., 2024) can all be seen as specialized forms of REU, each with a different emphasis.

In this work, we focus on three representative REU tasks: (i) REC, which targets single-object detection from complex reasoning queries; (ii) OVD, which addresses multi-object detection from template-based queries; and (iii) GRES, which requires multi-object segmentation from complex reasoning queries. All tasks are studied under few-shot settings. In our formulation, the number of shots refers to the number of annotated bounding boxes or masks. Specifically, in the FS-GREC setup, including FS-REC and FS-OVD, one ‘‘shot’’ is defined as an image–query–box triplet, while in FS-GRES, one ‘‘shot’’ corresponds to an image–query–mask triplet. Importantly, a ground-truth mask may include multiple valid instances for a single query (Li et al., 2025b). Among these tasks, FS-GRES is the most challenging, as it constitutes a pixel-level extension of FS-GREC and requires the model to generate accurate segmentation masks for objects described by natural-language queries in aerial images (Yuan et al., 2024).

The few-shot setting substantially increases task difficulty by requiring models to generalize from only a handful of labeled examples, in contrast to large-scale datasets such as VRSBench (Li et al., 2024b) (36k training examples), and DIOR-RSVG (27k) (Zhan et al., 2023). Few-shot REU is particularly challenging due to: (1) *visual diversity*, arising from large variations in object size, orientation, appearance, and inter-object relationships; and (2) *description diversity*, as natural language queries may vary in structure, vocabulary, abstraction level, and reasoning complexity. These factors jointly make few-shot REU a more realistic yet significantly harder problem compared to conventional large-scale training scenarios.

2.3 REWARD DESIGN

Following DeepSeek-R1, the reward function of Geo-R1 includes a task-agnostic format reward and a task-specific metrics reward.

2.3.1 FORMAT REWARD

To ensure reliable parsing and evaluation, the model’s output must follow a well-defined structure. We define a binary format reward that checks whether the response conforms to this structure. The output must be wrapped in reasoning tags `<think>...</think>` and `<answer>...</answer>`. The format reward is defined as:

$$R_{\text{format}}(q, o) = \begin{cases} 1, & \text{if output follows the expected format} \\ 0, & \text{otherwise} \end{cases} \quad (5)$$

2.3.2 METRICS REWARD

GREC. For the REC task, the VLM predicts a single object bounding box, i.e., $\mathbf{b}_{\text{pred}} = \mathcal{F}(I, q)$. An IoU reward can be calculated by comparing \mathbf{b}_{pred} with the ground-truth box \mathbf{b}_{gt} . For the OVD task, the VLM predicts is a set of box–label pairs, i.e., $\mathbb{B}_{\text{pred}} = \{(\mathbf{b}_{\text{pred}}^i, \mathbf{c}_{\text{pred}}^i)\}_{i=1}^N$, where $\mathbf{b}_{\text{pred}}^i$ denotes predicted bounding box, $\mathbf{c}_{\text{pred}}^i$ denotes category label. We then calculate reward as mAP between \mathbb{B}_{pred} and corresponding ground truth \mathbb{B}_{gt} , along with a penalty coefficient for overlength predictions. The metrics reward for GREC task is defined as follow:

$$R_{\text{metrics}}(q, o) = \begin{cases} \text{IoU}(\mathbf{b}_{\text{pred}}, \mathbf{b}_{\text{gt}}), & \text{for REC task} \\ \min(1, \sqrt{\frac{N_{\text{gt}}}{N}}) \cdot \text{mAP}(\mathbb{B}_{\text{pred}}, \mathbb{B}_{\text{gt}}), & \text{for OVD task} \end{cases} \quad (6)$$

where N_{gt} denotes the number of ground truth objects.

GRES. For GRES task, the VLM model is prompted to output a set of box–point pairs, $\mathbb{B}_{\text{pred}} = \{(b_{\text{pred}}^i, p_{\text{pred}}^i)\}_{i=1}^N$, where b_{pred}^i denotes a predicted bounding box and p_{pred}^i denotes the associated

keypoints. These predictions are then provided as prompts to a frozen SAM to generate final instance masks \mathbb{M}_{pred} . Each predicted instance mask is trimmed to ensure its boundary does not exceed that of the corresponding bounding box. Given ground truth instance masks \mathbb{M}_{gt} , the metrics reward for GRES task is defined as follows:

$$R_{\text{metrics}}(q, o) = \text{MaskGIoU}(\mathbb{M}_{\text{pred}}, \mathbb{M}_{\text{gt}}). \quad (7)$$

We follow LISA (Lai et al., 2024) to calculate mask GIoU.

3 MAIN EXPERIMENT

3.1 EXPERIMENT SETUP

Datasets. Unlike conventional few-shot learning (e.g., TPN (Liu et al., 2018) and DPGN (Yang et al., 2020)), we do not partition the dataset into base and novel classes. Instead, we treat all classes as novel and provide only a few labeled examples per class. We construct instruction-following few-shot datasets for the FS-GREC and FS-GRES tasks by deriving them from the training sets of three widely used remote sensing benchmarks: VRSBench Li et al. (2024b), NWPU VHR-10 (Cheng et al., 2014), and EarthReason (Li et al., 2025b). Configurations and statistics are summarized in Table 1. The term “shot” follows the definition in section 2.2. For the OVD task, we select four classes on which the baseline model (Qwen2.5-VL-3B) demonstrated decent performance. We select all categories from the training set for other tasks. The low-shot dataset is a subset of the high-shot dataset. To evaluate cross-dataset generalization, we further evaluate zero-shot performance on DIOR-RSVG (Zhan et al., 2023) and RRSIS-D (Yuan et al., 2024) datasets.

Table 1: Overview of our Few-Shot Referring Expression Understanding Datasets.

Dataset Name	Source Dataset	Task	# Categories	# Shots	# VQAs	# Images	Shot Definition
VRSBench-FS	VRSBench	FS-REC	26	{10, 5, 1}	260	254	image-query-box
NWPU-FS	NWPU VHR-10	FS-OVD	4	{10, 5}	25	25	image-query-box
EarthReason-FS	EarthReason	FS-GRES	24	{10, 5, 1}	240	240	image-query-mask

Model and Training Details. We adopt Qwen2.5-VL-3B-Instruct (Bai et al., 2025) as base model. Our implementation is built on the VLM-R1¹ and Easy-R1² codebase. Unless otherwise specified, we strictly inherit the default hyperparameters without manual tuning. We set the same batch size for different post-training paradigm. We trained comparing models for 30 epochs, with early stopping when the reward converged. All experiments are conducted on $8 \times \text{H100}$ GPUs, and a full training run takes approximately 10 to 20 hours. Prompt templates are shown in Appendix C. We apply thinking prompts for RL-based Paradigms. We adopt GRPO as our primary RL-based post-training paradigm. For SFT-based post-training, we perform visual instruction tuning with standard next token prediction (NTP) loss, implemented via LLaMA-Factory (Zheng et al., 2024).

3.2 FEW-SHOT GENERALIZED REFERRING EXPRESSION COMPREHENSION - REC

Task Evaluation. Performance on the REC subtask is measured by $\text{Acc}@_{\tau}$ (a prediction is correct if its box IoU with the ground truth exceeds τ) in the test set of VRSBench. We report metrics for $\text{Acc}@0.5$ and $\text{Acc}@0.7$. The experiments are conducted in 1-shot, 5-shot, and 10-shot configurations, with “Unique,” “Non-Unique,” and overall results reported. This evaluation compares the SFT method against two RL-based approaches, GRPO (Shao et al., 2024) and DAPO (Yu et al., 2025). We highlight the performance gap in red.

Results. Table 2 compares models trained on the full VRSBench (Full Amount Fine-tune) against few-shot models (1/5/10-shot Fine-tune). The few-shot results include both SFT-based models and our RL-tuned models. Performance data for the full-data baselines (except Qwen2.5-VL) are taken from the original VRSBench paper. The results reveal a clear performance hierarchy: RL-based post-training methods consistently and significantly outperform the SFT approach across all settings and metrics. This advantage is substantial; for example, in the 10-shot overall setting, our GRPO-based model achieves an $\text{Acc}@0.5$ score 12.30% higher than its SFT counterpart. Remarkably,

¹<https://github.com/om-ai-lab/VLM-R1>

²<https://github.com/hiyoga/EasyR1>

Table 2: Performance on VRSBench-FS for the FS-REC task. We report grounding accuracy at IoU thresholds of 0.5 and 0.7. Unique and Non-Unique indicate whether a referred object is the only instance of its category in the image or not.

Method	Base LLM	Unique		Non-Unique		Overall	
		Acc@0.5	Acc@0.7	Acc@0.5	Acc@0.7	Acc@0.5	Acc@0.7
Full Amount Fine-tune (36,313 samples)							
LLaVA-1.5 (Liu et al., 2024b)	Vicuna1.5-7B	51.10	16.40	34.80	11.50	41.60	13.60
Mini-Gemini (Li et al., 2024e)	Gemma-7B	41.10	9.60	22.30	4.90	30.10	6.80
MiniGPT-v2 (Chen et al., 2023)	Vicuna1.5-7B	40.70	18.90	32.40	15.20	35.80	16.80
GeoChat (Kuckreja et al., 2024)	Vicuna1.5-7B	57.40	22.60	44.50	18.00	49.80	19.90
Qwen2.5-VL (Bai et al., 2025)	Qwen2.5-3B	66.54	36.77	60.32	36.30	62.91	36.50
Zero-shot Baseline							
GPT-4V (OpenAI, 2024)	GPT-4	8.60	2.20	2.50	0.40	5.10	1.10
Qwen2.5-VL w/o thinking	Qwen2.5-3B	43.10	25.10	33.46	18.01	37.48	20.97
Qwen2.5-VL w/ thinking	Qwen2.5-3B	46.18	26.90	35.22	18.87	39.79	22.22
1-shot Fine-tune (26 samples)							
Qwen2.5-VL-SFT	Qwen2.5-3B	34.32	18.87	31.62	16.35	32.75	17.40
Geo-R1 (GRPO)	Qwen2.5-3B	52.17 (+17.85)	31.18 (+12.31)	41.21 (+9.59)	23.04 (+6.69)	45.78 (+12.03)	26.43 (+9.03)
Geo-R1 (DAPO)	Qwen2.5-3B	51.72 (+17.40)	31.68 (+12.81)	42.13 (+10.51)	24.50 (+8.15)	46.13 (+13.38)	27.50 (+10.10)
5-shot Fine-tune (130 samples)							
Qwen2.5-VL-SFT	Qwen2.5-3B	36.98	16.61	33.94	17.17	35.21	16.94
Geo-R1 (GRPO)	Qwen2.5-3B	54.11 (+17.13)	31.35 (+14.74)	42.98 (+9.04)	23.98 (+6.81)	47.62 (+12.41)	27.06 (+10.12)
Geo-R1 (DAPO)	Qwen2.5-3B	55.73 (+18.75)	32.19 (+15.58)	44.19 (+10.25)	24.86 (+7.69)	49.00 (+13.79)	27.92 (+10.98)
10-shot Fine-tune (260 samples)							
Qwen2.5-VL-SFT	Qwen2.5-3B	41.81	18.59	35.78	17.20	38.29	17.78
Geo-R1 (GRPO)	Qwen2.5-3B	57.27 (+15.46)	35.61 (+17.02)	45.81 (+10.03)	27.03 (+9.83)	50.59 (+12.30)	30.61 (+12.83)
Geo-R1 (DAPO)	Qwen2.5-3B	59.49 (+17.68)	37.11 (+18.52)	47.91 (+12.13)	28.07 (+10.87)	52.74 (+14.45)	31.84 (+14.06)

our 10-shot GRPO model using only 260 samples, 0.71% data, achieves a score that surpasses all evaluated models (except Qwen2.5-VL) trained on all 36,313 samples.

Within RL-based approaches, DAPO consistently outperforms GRPO across nearly all scenarios, indicating that more effective RL training could further enhance performance in few-shot settings. Moreover, the gains from RL-based methods are more pronounced on the Unique subset than on the Non-Unique subset, suggesting that RL approaches provide a larger boost on simpler tasks that do not require distinguishing between same-category distractors.

3.2.1 FEW-SHOT GENERALIZED REFERRING EXPRESSION COMPREHENSION - OVD

Task Evaluation. For the OVD task, we evaluate performance using the COCO-style mean Average Precision (mAP) in the test set of NWPU VHR-10 (Cheng et al., 2014). Our evaluation compares the SFT method against our GRPO approach. Experiments are run in 5/10-shot settings. Results are reported for the following four categories: airplane (PL), ship (SH), ground track field (GTF), and vehicle (VH). We intentionally exclude the 1-shot setting because training on a single instance would bias the model toward predicting a single instance per image, creating an inconsistency between the training and testing sets.

Results. Table 3 presents the OVD performance of SFT and GRPO tuned models. A notable observation is that SFT can be detrimental with extremely limited data. In both 10-shot and 5-shot settings, SFT-based models fail to surpass the performance of the zero-shot baseline in three out of four categories (airplane, ship, and vehicle). This suggests that the limited training data lacks intra-class diversity, causing the model to memorize the specific and even spurious features of the few samples rather than the general concept of the class, leading to overfitting, degrading the model’s detection capabilities. In contrast, the GRPO-tuned model consistently outperforms the SFT model across all categories and settings, demonstrating that RL is more efficient for learning OVD from a few exam-

Table 3: Performance on FS-NWPU for the FS-OVD task. We report mAP in COCO style.

	PL	SH	GTF	VH	Avg.
Zero-shot Baseline					
Qwen2.5-VL w/o thinking	23.79	25.34	44.13	24.04	29.33
Qwen2.5-VL w/ thinking	25.17	21.85	57.08	23.95	32.01
5-shot Fine-tune (20 samples)					
Qwen2.5-VL-SFT	6.32	22.33	65.48	12.36	26.62
Geo-R1 (GRPO)	21.74	25.42	70.23	15.40	33.20
10-shot Fine-tune (40 samples)					
Qwen2.5-VL-SFT	15.76	21.90	68.42	14.73	30.20
Geo-R1 (GRPO)	25.76	28.12	69.24	16.57	34.92

ples. More importantly, the advantage of GRPO becomes even more critical in the more challenging low-data setting. The performance gap between GRPO and SFT increases from 4.72 mAP in the 10-shot scenario to 6.58 mAP in the 5-shot scenario. This widening margin highlights GRPO’s ability to learn effectively in data-scarce environments where SFT struggles.

3.2.2 FEW-SHOT GENERALIZED REFERRING EXPRESSION SEGMENTATION

Task Evaluation. We conduct experiments on the EarthReason (Li et al., 2025b) dataset under few-shot setting. Following LISA (Lai et al., 2024), performance on the GRES task is measured by the mask-based gIoU, defined by the average of all per-image IoUs. We use this metric because alternatives like cIoU are highly biased toward large-area objects and tend to fluctuate significantly. We report the final gIoU scores on the validation and test sets of the EarthReason dataset.

Results. In Table 4, we demonstrate the effective results of our proposed pipeline and task-specific reward for training reasoning models of FS-GRES task. A direct performance comparison with SFT-tuned model like in FS-GREC tasks is not feasible due to the unique bbox-mask-reward pipeline. To establish a fair benchmark, we compare our method against SegEarth-R1, which is trained using SegEarth-R1 pipeline on the same limited datasets EarthReason-FS. First, we found our GRPO-trained model, i.e., Geo-R1, demonstrates a significant improvement compared to the zero-shot baseline. It achieves a gIoU increase of up to 38.48 points on the validation set (from 19.35 to 57.78) and up to 26.11 points on the test set (from 32.16 to 58.27), showing the success of RL-based post-training paradigm. Then, we observe the model exhibits remarkable performance with a very small number of samples. With just 240 samples (10-shot), our model demonstrates a comparable performance with PixelLM, which are trained on 900K instances with descriptions. *Using only 240 samples (10-shot), which is roughly 2% training data, Geo-R1 reaches nearly 83% of the performance of the SegEarth-R1 model that was trained on the entire training set.*

In a direct comparison, the GRPO pipeline consistently yields superior models to the SFT approach. Geo-R1 outperforms SegEarth-R1 in both the 10-shot and 5-shot settings. Crucially, *this performance gap becomes more significant as the amount of training data decreases.* This trend indicates that RL-based post-training paradigm is a more effective and sample-efficient method for adapting large VLM to this specialized, pixel-level task, especially in data-scarce scenarios.

Table 4: Performance on the EarthReason for the FS-RES task. We report gIoU.

	Val	Test
Full Amount Fine-tune		
LISA	61.04	60.88
PixelLM	57.94	60.01
PSALM	66.61	68.30
SegEarth-R1	68.60	70.75
Zero-shot Baseline		
Qwen2.5-VL w/ thinking	19.35	32.16
1-shot Fine-tune (24 samples)		
SegEarth-R1	42.47	43.01
Geo-R1	51.38	50.30
5-shot Fine-tune (120 samples)		
SegEarth-R1	45.37	45.46
Geo-R1	54.73	56.01
10-shot Fine-tune (240 samples)		
SegEarth-R1	56.40	56.60
Geo-R1	57.78	58.27

4 DISCUSSION

In this section, we first compare the learning dynamics of SFT and GRPO, then examine cross-dataset generalization, the upper bound of few-shot learning, and the impact of model size. Unless otherwise specified, experiments are conducted on the VRSBench-FS dataset under the 10-shot setting.

4.1 LEARNING CURVE COMPARISON

We fine-tune Qwen2.5-VL-3B with both SFT and GRPO on the FS-REC task using same batch size and evaluate checkpoints every 100 steps to sketch the learning curve. As shown in Figure 2, GRPO consistently outperforms SFT at every checkpoint, with an average gain of 9.74%. GRPO improves steadily, peaking around 400 steps, and remains strong until the end, whereas SFT oscillated within 37%–40%. GRPO achieves a clearly higher ceiling and stabilizes around 50%, indicating better training efficiency under few-shot setting.

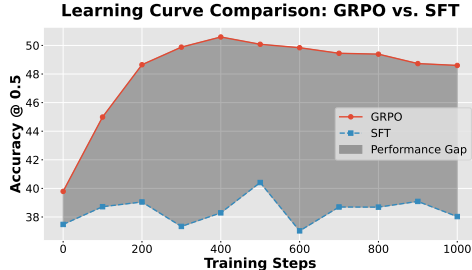


Figure 2: Learning curves of GRPO vs. SFT on FS-REC.

4.2 CROSS DATASET GENERALIZATION

We further assess the cross-dataset generalization of the SFT and GRPO approaches on the FS-GREC and FS-GRES tasks. For the FS-GREC task, we fine-tune models on the VRSBench dataset with limited supervision (1, 5, and 10-shot) and then evaluate model performance on the DIOR-RSVG target dataset, in a zero-shot manner. As shown in Table 5, GRPO consistently outperforms SFT across all settings, achieving a performance advantage of 4.92%, 6.05%, and 5.52% in the 1-shot, 5-shot, and 10-shot scenarios, respectively.

Table 5: Cross Dataset Evaluation.

	VRSBench → DIOR-RSVG		EarthReason → RRSIS-D	
# shot	SegEarth-R1	Geo-R1	SegEarth-R1	Geo-R1
1-shot	32.35	37.27 (+4.92)	18.77	32.11 (+13.34)
5-shot	34.52	40.57 (+6.05)	20.29	36.41 (+16.12)
10-shot	34.86	40.38 (+5.52)	24.27	37.83 (+13.56)

Similarly, for the FS-GRES task, models were tuned on the EarthReason dataset (1, 5, and 10-shot) and tested on the RRSIS-D dataset. Here, the GRPO-based model (Geo-R1) demonstrates a remarkable improvement over the SFT-based model (SegEarth-R1) under few-shot setting, achieving a relative improvement up to 80%. These results highlight GRPO’s incredible cross-dataset generalization, indicating superior transferability and robustness of Geo-R1.

4.3 UPPER BOUND OF FEW-SHOT LEARNING

As shown in Figure 3, GRPO clearly outperforms SFT in low-shot settings, although this performance gap narrows as supervision increases. To investigate this trend and determine the upper-bound capability of Geo-R1, we experimented with additional shot numbers (20, 50, 100, and 200). Concretely, the margin between GRPO and SFT approaches shrinks from 13.03% at 1-shot to 0.47% at 200-shot. This diminishing advantage suggests both approaches approach a common upper bound with more data. Empirically, they converge toward the full-data SFT result of 62.91%, indicating GRPO’s strong sample efficiency at small shots but similar asymptotic performance as shot count grows.

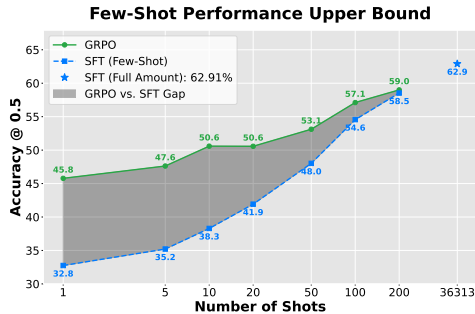


Figure 3: Few-shot Learning Upper-Bound.

4.4 FEW-SHOT LEARNING MEETS MODEL SIZE

We then examine how model size influences the performance under different post-training paradigms. As shown in Figure 4, both SFT and GRPO benefit from increased model scales. However, this trend exhibits clear diminishing marginal returns. For instance, SFT gains 4.31% when scaling from 3B to 7B but only 2.23% from 7B to 32B, with a similar slowdown observed for GRPO from 3B to 7B. This suggests that while larger models provide a stronger foundation, simply increasing number of parameters yields limited benefits for the few-shot task. This can be attributed to the limited fine-tuning data. With few examples, high-capacity models tend to overfit by simply memorizing the training samples rather than learning generalizable features. Notably, GRPO’s performance decreased on the 32B model, likely due to two factors: overfitting on limited data and numerical instability from bf16 training.

GRPO vs. SFT Performance by Model Size (REC 10-shot)

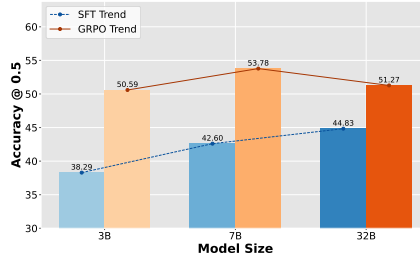


Figure 4: Few-shot Learning Upper-Bound.

5 RELATED WORK

Reasoning LLMs and VLMs. The OpenAI o1 (Jaech et al., 2024) showed that RL improves the reasoning capability of LLMs by learning from feedback on final outcomes. Recently, DeepSeek-R1 (Guo et al., 2025) demonstrated that rule-based rewards can be used with the GRPO algorithm to teach LLMs advanced reasoning skills. Inspired by the success of RL in LLMs, researchers are now applying the R1 framework to VLMs. R1-OneVision (Yang et al., 2025) created a step-by-step multimodal reasoning datasets for SFT and RL. Concurrently, R1-V (Chen et al., 2025) applied the GRPO algorithm to object counting, achieving the remarkable result of a 3B model outperforming much larger 72B models. VisualThinker-R1-Zero (Zhou et al., 2025) applied it directly to base VLMs, observing “visual aha moments”. Other studies refined the training process: Vision-R1 (Huang et al., 2025) first created a multimodal CoT dataset, serving as a cold-start before RL; LMM-R1 (Peng et al., 2025) used a two-phase strategy, starting with text-only reasoning before fine-tuning on multimodal data. Visual-RFT (Liu et al., 2025b), VLM-R1 (Shen et al., 2025), and Seg-Zero (Liu et al., 2025a) explored applying RL to image perception tasks.

Few-shot Learning in Remote Sensing. Few-shot learning (FSL) is crucial in RS, since it effectively addresses the challenge of limited labeled data. Attention-based contrastive learning have been shown to significantly improve classification accuracy in scene classification tasks (Xu et al., 2024; Zeng & Geng, 2022). Prototype-based networks (Li et al., 2021; Cheng et al., 2022) and multi-scale feature fusion strategies (Zhao et al., 2022) help models obtain diverse object characteristics, achieving state-of-the-art results on RS object detection benchmarks under few-shot settings. For segmentation, adaptive prototype clustering and mask-guided correlation learning enable precise pixel-level interpretation even with few annotated samples (Jiang et al., 2022; Jia et al., 2025; Li et al., 2024a; Shen et al., 2024). FSL enhances the efficiency and interpretability of RSI analysis, while also addressing key challenges in generalization and multimodal integration (Sun et al., 2021; Lee et al., 2024).

REC and RES in Remote Sensing. Referring expression comprehension in remote sensing—often termed remote sensing visual grounding (RSVG), which localizes a target in aerial imagery from a natural-language description. Early progress was established by the RSVG benchmark and the GeoVG model (Sun et al., 2022), and extended by DIOR-RSVG to broaden categories and scene scale (Zhan et al., 2023). In the MLLM era, GeoChat (Kuckreja et al., 2024) was the first MLLM to handle a wide range of RS vision-language tasks, including RSVG. Later, VRSBench (Li et al., 2024b) provided a high-quality dataset for RSVG task. RS-specific MLLMs such as EarthGPT (Zhang et al., 2024), RSGPT (Hu et al., 2025), SkySenseGPT (Luo et al., 2024), VHM (Pang et al., 2025), further unified different vision-language tasks, such as captioning, VG, VQA, and OVD, thus improving RS-specific alignment. For RES, Yuan et al. introduced the RES task for RS and released the RefSegRS dataset (Yuan et al., 2024). Liu et al. later introduced RRSIS-D, enabling pixel-level referring at scale (Liu et al., 2024c). Recent works such as GeoGround (Zhou et al., 2024b) and Skysense-O (Zhu et al., 2025) further unified the REC and RES tasks for RS images. Besides, works for OVD (Li et al., 2024d; Pan et al., 2025), and OVS (Li et al., 2025a;b) can be

viewed as a special case of REC and RES (locate multiple objects with template-based description), which support grounding of novel categories.

6 CONCLUSION

In this paper, we define a generic task, Referring Expression Understanding, and contribute three corresponding few-shot remote sensing datasets for training: VRSBench-FS, NWPU-FS, and EarthReason-FS. We then compare RL-based (GRPO) and SFT-based post-training paradigms on few-shot REC, OVD, and GRES tasks within the RS domain. Our results show that our GRPO-trained model, Geo-R1, consistently outperforms standard SFT-tuned models across these tasks. The performance gains are particularly large in low-shot regimes, and the model exhibits significantly stronger cross-dataset generalization.

While our study demonstrates the effectiveness of reinforcement learning for few-shot referring expression understanding, several avenues remain. Our evaluation is limited to high-resolution aerial imagery; extending Geo-R1 to multispectral (e.g., Sentinel-2) and SAR data would further test its robustness. Beyond the three REU tasks studied (REC, RES, OVD), future work could explore broader grounding tasks such as GREC and OVS. Finally, scaling to larger shots, refining reward functions, and designing powerful RL training recipes remain promising directions.

REFERENCES

- Shuai Bai, Keqin Chen, Xuejing Liu, Jialin Wang, Wenbin Ge, Sibao Song, Kai Dang, Peng Wang, Shijie Wang, Jun Tang, Humen Zhong, Yuanzhi Zhu, Mingkun Yang, Zhaohai Li, Jianqiang Wan, Pengfei Wang, Wei Ding, Zheren Fu, Yiheng Xu, Jiabo Ye, Xi Zhang, Tianbao Xie, Zesen Cheng, Hang Zhang, Zhibo Yang, Haiyang Xu, and Junyang Lin. Qwen2.5-vl technical report. *arXiv preprint arXiv:2502.13923*, 2025.
- Jun Chen, Deyao Zhu, Xiaoqian Shen, Xiang Li, Zechun Liu, Pengchuan Zhang, Raghuraman Krishnamoorthi, Vikas Chandra, Yunyang Xiong, and Mohamed Elhoseiny. Minigpt-v2: large language model as a unified interface for vision-language multi-task learning. *arXiv preprint arXiv:2310.09478*, 2023.
- Liang Chen, Lei Li, Haozhe Zhao, Yifan Song, and Vinci. R1-v: Reinforcing super generalization ability in vision-language models with less than \$3. <https://github.com/Deep-Agent/R1-V>, 2025. Accessed: 2025-02-02.
- Gong Cheng, Junwei Han, Peicheng Zhou, and Lei Guo. Multi-class geospatial object detection and geographic image classification based on collection of part detectors. *ISPRS Journal of Photogrammetry and Remote Sensing*, 98:119–132, 2014.
- Gong Cheng, Bowei Yan, Peizhen Shi, Ke Li, Xiwen Yao, Lei Guo, and Junwei Han. Prototype-cnn for few-shot object detection in remote sensing images. *IEEE Transactions on Geoscience and Remote Sensing*, 60:1–10, 2022. doi: 10.1109/TGRS.2021.3078507.
- Daya Guo, Dejian Yang, Haowei Zhang, Junxiao Song, Peiyi Wang, Qihao Zhu, Runxin Xu, Ruoyu Zhang, Shirong Ma, Xiao Bi, et al. Deepseek-r1 incentivizes reasoning in llms through reinforcement learning. *Nature*, 645(8081):633–638, 2025.
- Shuting He, Henghui Ding, Chang Liu, and Xudong Jiang. Grec: Generalized referring expression comprehension. *arXiv preprint arXiv:2308.16182*, 2023.
- Yuan Hu, Jianlong Yuan, Congcong Wen, Xiaonan Lu, Yu Liu, and Xiang Li. Rsgpt: A remote sensing vision language model and benchmark. *ISPRS Journal of Photogrammetry and Remote Sensing*, 224:272–286, 2025.
- Wenxuan Huang, Bohan Jia, Zijie Zhai, Shaosheng Cao, Zheyu Ye, Fei Zhao, Yao Hu, and Shaohui Lin. Vision-r1: Incentivizing reasoning capability in multimodal large language models. *arXiv preprint arXiv:2503.06749*, 2025.
- Aaron Jaech, Adam Kalai, Adam Lerer, Adam Richardson, Ahmed El-Kishky, Aiden Low, Alec Helyar, Aleksander Madry, Alex Beutel, Alex Carney, et al. Openai o1 system card. *arXiv preprint arXiv:2412.16720*, 2024.
- Yuyu Jia, Jiabo Li, and Qi Wang. Generalized few-shot semantic segmentation for remote sensing images. *IEEE Transactions on Geoscience and Remote Sensing*, 63:1–10, 2025. doi: 10.1109/TGRS.2025.3531874.
- Xufeng Jiang, Nan Zhou, and Xiang Li. Few-shot segmentation of remote sensing images using deep metric learning. *IEEE Geoscience and Remote Sensing Letters*, 19:1–5, 2022.
- Kartik Kuckreja, Muhammad S Danish, Muzammal Naseer, Abhijit Das, Salman Khan, and Fahad S Khan. Geochat: Grounded large vision-language model for remote sensing. the iee. In *CVF Conference on Computer Vision and Pattern Recognition*, volume 2, pp. 4, 2024.
- Xin Lai, Zhuotao Tian, Yukang Chen, Yanwei Li, Yuhui Yuan, Shu Liu, and Jiaya Jia. Lisa: Reasoning segmentation via large language model. In *Proceedings of the IEEE/CVF Conference on Computer Vision and Pattern Recognition (CVPR)*, pp. 9579–9589, June 2024.
- Gao Yu Lee, Tanmoy Dam, Md Meftahul Ferdous, Daniel Puiu Poenar, and Vu N Duong. Unlocking the capabilities of explainable few-shot learning in remote sensing. *Artificial Intelligence Review*, 57(7):169, 2024.

- Kaiyu Li, Ruixun Liu, Xiangyong Cao, Xueru Bai, Feng Zhou, Deyu Meng, and Zhi Wang. Segearth-ov: Towards training-free open-vocabulary segmentation for remote sensing images. In *Proceedings of the Computer Vision and Pattern Recognition Conference*, pp. 10545–10556, 2025a.
- Kaiyu Li, Zepeng Xin, Li Pang, Chao Pang, Yupeng Deng, Jing Yao, Guisong Xia, Deyu Meng, Zhi Wang, and Xiangyong Cao. Segearth-r1: Geospatial pixel reasoning via large language model. *arXiv preprint arXiv:2504.09644*, 2025b.
- Shuo Li, Fang Liu, Licheng Jiao, Xu Liu, Puhua Chen, and Lingling Li. Mask-guided correlation learning for few-shot segmentation in remote sensing imagery. *IEEE Transactions on Geoscience and Remote Sensing*, 62:1–14, 2024a. doi: 10.1109/TGRS.2024.3417965.
- Xiang Li, Jingyu Deng, and Yi Fang. Few-shot object detection on remote sensing images. *IEEE Transactions on Geoscience and Remote Sensing*, 60:1–14, 2021.
- Xiang Li, Congcong Wen, Yuan Hu, and Nan Zhou. Rs-clip: Zero shot remote sensing scene classification via contrastive vision-language supervision. *International Journal of Applied Earth Observation and Geoinformation*, 124:103497, 2023.
- Xiang Li, Jian Ding, and Mohamed Elhoseiny. Vrsbench: A versatile vision-language benchmark dataset for remote sensing image understanding. *Advances in Neural Information Processing Systems*, 37:3229–3242, 2024b.
- Xiang Li, Congcong Wen, Yuan Hu, Zhenghang Yuan, and Xiao Xiang Zhu. Vision-language models in remote sensing: Current progress and future trends. *IEEE Geoscience and Remote Sensing Magazine*, 12(2):32–66, 2024c.
- Yan Li, Weiwei Guo, Xue Yang, Ning Liao, Dunnyun He, Jiaqi Zhou, and Wenxian Yu. Toward open vocabulary aerial object detection with clip-activated student-teacher learning. In *European Conference on Computer Vision*, pp. 431–448. Springer, 2024d.
- Yanwei Li, Yuechen Zhang, Chengyao Wang, Zhisheng Zhong, Yixin Chen, Ruihang Chu, Shaoteng Liu, and Jiaya Jia. Mini-gemini: Mining the potential of multi-modality vision language models. *arXiv preprint arXiv:2403.18814*, 2024e.
- Chang Liu, Henghui Ding, and Xudong Jiang. Gres: Generalized referring expression segmentation. In *Proceedings of the IEEE/CVF conference on computer vision and pattern recognition*, pp. 23592–23601, 2023.
- Fan Liu, Delong Chen, Zhangqingyun Guan, Xiaocong Zhou, Jiale Zhu, Qiaolin Ye, Liyong Fu, and Jun Zhou. Remotepclip: A vision language foundation model for remote sensing. *IEEE Transactions on Geoscience and Remote Sensing*, 62:1–16, 2024a.
- Haotian Liu, Chunyuan Li, Yuheng Li, and Yong Jae Lee. Improved baselines with visual instruction tuning. In *2024 IEEE/CVF Conference on Computer Vision and Pattern Recognition (CVPR)*, pp. 26286–26296, 2024b.
- Sihan Liu, Yiwei Ma, Xiaoqing Zhang, Haowei Wang, Jiayi Ji, Xiaoshuai Sun, and Rongrong Ji. Rotated multi-scale interaction network for referring remote sensing image segmentation. In *2024 IEEE/CVF Conference on Computer Vision and Pattern Recognition (CVPR)*, pp. 26648–26658, 2024c.
- Yanbin Liu, Juho Lee, Minseop Park, Saehoon Kim, Eunho Yang, Sung Ju Hwang, and Yi Yang. Learning to propagate labels: Transductive propagation network for few-shot learning. In *International Conference on Learning Representations*, 2018.
- Yuqi Liu, Bohao Peng, Zhisheng Zhong, Zihao Yue, Fanbin Lu, Bei Yu, and Jiaya Jia. Seg-zero: Reasoning-chain guided segmentation via cognitive reinforcement. *arXiv preprint arXiv:2503.06520*, 2025a.
- Ziyu Liu, Zeyi Sun, Yuhang Zang, Xiaoyi Dong, Yuhang Cao, Haodong Duan, Dahua Lin, and Jiaqi Wang. Visual-rft: Visual reinforcement fine-tuning. *arXiv preprint arXiv:2503.01785*, 2025b.

- Junwei Luo, Zhen Pang, Yongjun Zhang, Tingzhu Wang, Linlin Wang, Bo Dang, Jiangwei Lao, Jian Wang, Jingdong Chen, Yihua Tan, et al. Skysensegpt: A fine-grained instruction tuning dataset and model for remote sensing vision-language understanding. *arXiv preprint arXiv:2406.10100*, 2024.
- OpenAI. Gpt-4v(ision) system card. https://cdn.openai.com/papers/GPTV_System_Card.pdf, 2024. Accessed: 2025-08-30.
- Jiancheng Pan, Yanxing Liu, Yuqian Fu, Muyuan Ma, Jiahao Li, Danda Pani Paudel, Luc Van Gool, and Xiaomeng Huang. Locate anything on earth: Advancing open-vocabulary object detection for remote sensing community. In *Proceedings of the AAAI Conference on Artificial Intelligence*, volume 39, pp. 6281–6289, 2025.
- Chao Pang, Xingxing Weng, Jiang Wu, Jiayu Li, Yi Liu, Jiaying Sun, Weijia Li, Shuai Wang, Litong Feng, Gui-Song Xia, et al. Vhm: Versatile and honest vision language model for remote sensing image analysis. In *Proceedings of the AAAI Conference on Artificial Intelligence*, volume 39, pp. 6381–6388, 2025.
- Yingzhe Peng, Gongrui Zhang, Miaosen Zhang, Zhiyuan You, Jie Liu, Qipeng Zhu, Kai Yang, Xingzhong Xu, Xin Geng, and Xu Yang. Lmm-r1: Empowering 3b lms with strong reasoning abilities through two-stage rule-based rl. *arXiv preprint arXiv:2503.07536*, 2025.
- Bryan A. Plummer, Liwei Wang, Chris M. Cervantes, Juan C. Caicedo, Julia Hockenmaier, and Svetlana Lazebnik. Flickr30k entities: Collecting region-to-phrase correspondences for richer image-to-sentence models. In *2015 IEEE International Conference on Computer Vision (ICCV)*, pp. 2641–2649, 2015. doi: 10.1109/ICCV.2015.303.
- Alec Radford, Jong Wook Kim, Chris Hallacy, Aditya Ramesh, Gabriel Goh, Sandhini Agarwal, Girish Sastry, Amanda Askell, Pamela Mishkin, Jack Clark, et al. Learning transferable visual models from natural language supervision. In *International conference on machine learning*, pp. 8748–8763. PmlR, 2021.
- Nikhila Ravi, Valentin Gabeur, Yuan-Ting Hu, Ronghang Hu, Chaitanya Ryali, Tengyu Ma, Haitham Khedr, Roman Rädle, Chloe Rolland, Laura Gustafson, Eric Mintun, Junting Pan, Kalyan Vasudev Alwala, Nicolas Carion, Chao-Yuan Wu, Ross Girshick, Piotr Dollar, and Christoph Feichtenhofer. SAM 2: Segment anything in images and videos. In *The Thirteenth International Conference on Learning Representations*, 2025.
- John Schulman, Filip Wolski, Prafulla Dhariwal, Alec Radford, and Oleg Klimov. Proximal policy optimization algorithms. *arXiv preprint arXiv:1707.06347*, 2017.
- Zhihong Shao, Peiyi Wang, Qihao Zhu, Runxin Xu, Junxiao Song, Xiao Bi, Haowei Zhang, Mingchuan Zhang, YK Li, Yang Wu, et al. Deepseekmath: Pushing the limits of mathematical reasoning in open language models. *arXiv preprint arXiv:2402.03300*, 2024.
- Haozhan Shen, Peng Liu, Jingcheng Li, Chunxin Fang, Yibo Ma, Jiajia Liao, Qiaoli Shen, Zilun Zhang, Kangjia Zhao, Qianqian Zhang, et al. Vlm-r1: A stable and generalizable r1-style large vision-language model. *arXiv preprint arXiv:2504.07615*, 2025.
- Weihao Shen, Ailong Ma, Junjue Wang, Zhuo Zheng, and Yanfei Zhong. Adaptive self-supporting prototype learning for remote sensing few-shot semantic segmentation. *IEEE Transactions on Geoscience and Remote Sensing*, 62:1–16, 2024. doi: 10.1109/TGRS.2024.3435086.
- Xian Sun, Bing Wang, Zhirui Wang, Hao Li, Hengchao Li, and Kun Fu. Research progress on few-shot learning for remote sensing image interpretation. *IEEE Journal of Selected Topics in Applied Earth Observations and Remote Sensing*, 14:2387–2402, 2021. doi: 10.1109/JSTARS.2021.3052869.
- Yuxi Sun, Shanshan Feng, Xutao Li, Yunming Ye, Jian Kang, and Xu Huang. Visual grounding in remote sensing images. In *Proceedings of the 30th ACM International Conference on Multimedia*, MM '22, pp. 404–412, New York, NY, USA, 2022. Association for Computing Machinery. ISBN 9781450392037. doi: 10.1145/3503161.3548316.

- Xingxing Weng, Chao Pang, and Gui-Song Xia. Vision-language modeling meets remote sensing: Models, datasets, and perspectives. *IEEE Geoscience and Remote Sensing Magazine*, 2025.
- Jianzong Wu, Xiangtai Li, Shilin Xu, Haobo Yuan, Henghui Ding, Yibo Yang, Xia Li, Jiangning Zhang, Yunhai Tong, Xudong Jiang, et al. Towards open vocabulary learning: A survey. *IEEE Transactions on Pattern Analysis and Machine Intelligence*, 46(7):5092–5113, 2024.
- Yulong Xu, Hanbo Bi, Hongfeng Yu, Wanxuan Lu, Peifeng Li, Xinming Li, and Xian Sun. Attention-based contrastive learning for few-shot remote sensing image classification. *IEEE Transactions on Geoscience and Remote Sensing*, 62:1–17, 2024. doi: 10.1109/TGRS.2024.3385655.
- Ling Yang, Liangliang Li, Zilun Zhang, Xinyu Zhou, Erjin Zhou, and Yu Liu. Dpgn: Distribution propagation graph network for few-shot learning. In *Proceedings of the IEEE/CVF Conference on Computer Vision and Pattern Recognition (CVPR)*, June 2020.
- Yi Yang, Xiaoxuan He, Hongkun Pan, Xiyan Jiang, Yan Deng, Xingtao Yang, Haoyu Lu, Dacheng Yin, Fengyun Rao, Minfeng Zhu, et al. R1-onevision: Advancing generalized multimodal reasoning through cross-modal formalization. *arXiv preprint arXiv:2503.10615*, 2025.
- Qiyang Yu, Zheng Zhang, Ruofei Zhu, Yufeng Yuan, Xiaochen Zuo, Yu Yue, Weinan Dai, Tiantian Fan, Gaohong Liu, Lingjun Liu, et al. Dapo: An open-source llm reinforcement learning system at scale. *arXiv preprint arXiv:2503.14476*, 2025.
- Zhenghang Yuan, Lichao Mou, Yuansheng Hua, and Xiao Xiang Zhu. Rrsis: Referring remote sensing image segmentation. *IEEE Transactions on Geoscience and Remote Sensing*, 2024.
- Qingjie Zeng and Jie Geng. Task-specific contrastive learning for few-shot remote sensing image scene classification. *ISPRS Journal of Photogrammetry and Remote Sensing*, 191:143–154, 2022.
- Yang Zhan, Zhitong Xiong, and Yuan Yuan. Rsvg: Exploring data and models for visual grounding on remote sensing data. *IEEE Transactions on Geoscience and Remote Sensing*, 61:1–13, 2023.
- Wei Zhang, Miaoxin Cai, Tong Zhang, Yin Zhuang, and Xuerui Mao. Earthgpt: A universal multimodal large language model for multisensor image comprehension in remote sensing domain. *IEEE Transactions on Geoscience and Remote Sensing*, 62:1–20, 2024.
- Zhitao Zhao, Ping Tang, Lijun Zhao, and Zheng Zhang. Few-shot object detection of remote sensing images via two-stage fine-tuning. *IEEE Geoscience and Remote Sensing Letters*, 19:1–5, 2022. doi: 10.1109/LGRS.2021.3116858.
- Yaowei Zheng, Richong Zhang, Junhao Zhang, Yanhan Ye, Zheyang Luo, Zhangchi Feng, and Yongqiang Ma. Llamafactory: Unified efficient fine-tuning of 100+ language models. *arXiv preprint arXiv:2403.13372*, 2024.
- Hengguang Zhou, Xirui Li, Ruochen Wang, Minhao Cheng, Tianyi Zhou, and Cho-Jui Hsieh. R1-zero’s “aha moment” in visual reasoning on a 2b non-sft model. *arXiv preprint arXiv:2503.05132*, 2025.
- Yue Zhou, Litong Feng, Yiping Ke, Xue Jiang, Junchi Yan, Xue Yang, and Wayne Zhang. Towards vision-language geo-foundation model: A survey. *arXiv preprint arXiv:2406.09385*, 2024a.
- Yue Zhou, Mengcheng Lan, Xiang Li, Litong Feng, Yiping Ke, Xue Jiang, Qingyun Li, Xue Yang, and Wayne Zhang. Geoground: A unified large vision-language model for remote sensing visual grounding. *arXiv preprint arXiv:2411.11904*, 2024b.
- Qi Zhu, Jiangwei Lao, Deyi Ji, Junwei Luo, Kang Wu, Yingying Zhang, Lixiang Ru, Jian Wang, Jingdong Chen, Ming Yang, Dong Liu, and Feng Zhao. Skysense-o: Towards open-world remote sensing interpretation with vision-centric visual-language modeling. In *Proceedings of the Computer Vision and Pattern Recognition Conference (CVPR)*, pp. 14733–14744, June 2025.

A THE USE OF LARGE LANGUAGE MODELS

The LLMs were used in three ways: (i) to edit and polish grammar and phrasing; (ii) using “Deep-Research” to help retrieve and cluster related literature (with all citations verified by the authors). We reviewed, verified, and take full responsibility for the contents.

B REPRODUCIBILITY STATEMENT

We are committed to ensuring the reproducibility of our research. When we trained the SFT model, GRPO model and DAPO model, all the random seeds are fixed. Our implementation is built upon VLM-R1 and Easy-R1 codebase. All datasets used in our experiments, such as VRSBench, NWPU, EarthReason, RRSIS-D, and DIOR-RSVG, are publicly available. All models, training recipes will be open-sourced in <http://geo-r1.github.io> to make sure the results presented in our main paper are reproducible.

C PROMPT TEMPLATE

We largely follow the VLM-R1 prompt templates for REC, OVD, and extend the same interface to the GRES setting. We append the thinking template at the end for all task prompts.

Prompt Template of REC

Please provide the bounding box coordinates of the region this sentence describes: {query}.

Prompt Template of OVD

Please carefully check the image and detect the following objects: {target list}. Output each detected target's bbox coordinates in JSON format. The format of the bbox coordinates is:

```
```json
[
 {
 "bbox_2d": [x1, y1, x2, y2],
 "label": "category name"
 },
 {
 "bbox_2d": [x1, y1, x2, y2],
 "label": "category name"
 }
]
```
```

If there are no such targets in the image, simply respond with None.

Prompt Template of GRES

Please carefully check the image and answer: {query}. Based on your answer, detect all relevant objects in the image. Output each detected target's bbox coordinates in JSON format. The format of the bbox coordinates is:

```
```json
[
 {
 "bbox_2d": [x1, y1, x2, y2],
 "keypoint1": [x3, y3],
 "keypoint2": [x4, y4]
 },
 {
 "bbox_2d": [x1, y1, x2, y2],
 "keypoint1": [x3, y3],
 "keypoint2": [x4, y4]
 }
]
```
```

Thinking Template

{problem} Output the thinking process in <think> </think> and final answer in <answer> </answer> tags.

D DEMO

We visualize the model's reasoning process for demonstration. Figure 5 shows some successful case on GRES task, while Figure 6 illustrates examples on GREC tasks. In general, Geo-R1 is able to provide a reasonable thinking process that leads to the accurate answer.

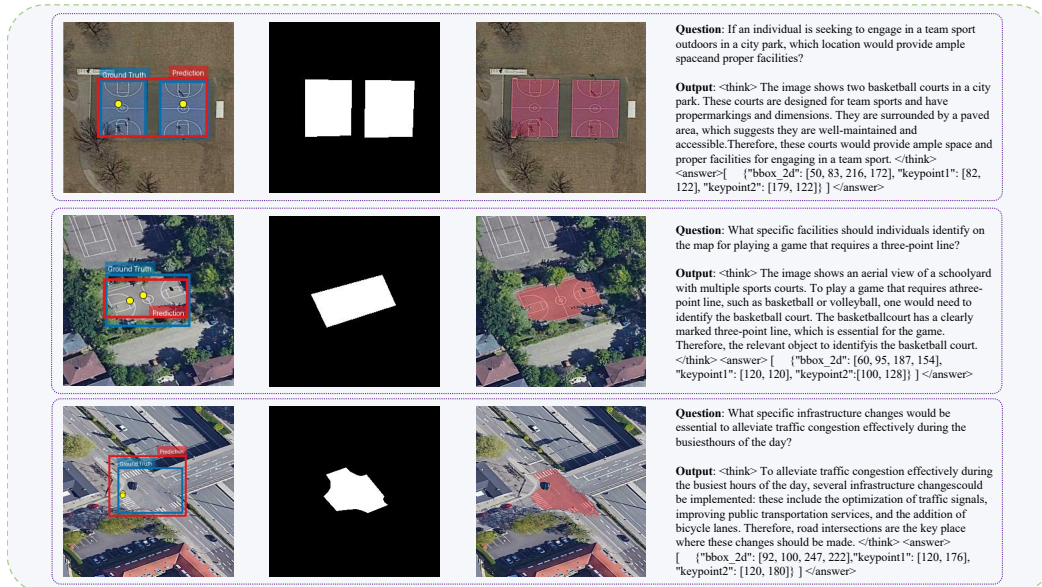


Figure 5: Geo-R1 inference samples (success case for GRES).

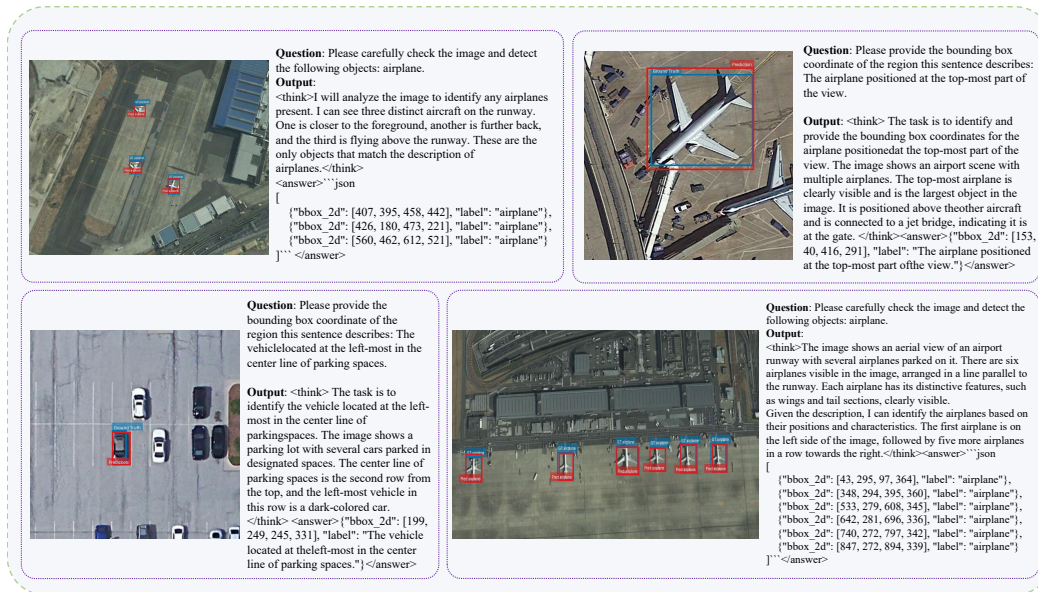


Figure 6: Geo-R1 inference samples (success case for GREC).

In general, Geo-R1 is able to provide a reasonable thinking process that leads to an accurate answer. However, we also identify key failure modes that highlight a disconnect between an often-plausible reasoning process and the final spatial output.

As shown in the top-left of Figure 7, the model can correctly reason in its reasoning process that the park area is the most suitable region for wildlife preservation, yet its final answer incorrectly grounds this concept to the nearby sports facility. In the bottom-right example, the model’s reasoning correctly identifies the presence of multiple ships, but the final answer detects only the cluster on the left while omitting the group on the right. Furthermore, we also observe failures in reasoning process, the bottom-left example shows a failure within the reasoning process itself. Although the model accurately understands the task in its reasoning block (to identify the ‘large vehicle’), it subsequently fails to apply this critical size attribute, incorrectly selecting a much smaller, adjacent vehicle for its final answer. These cases suggest that a key area for future improvement is strengthening the alignment between the model’s high-level semantic understanding and the generation of accurate, complete, and precise spatial coordinates.

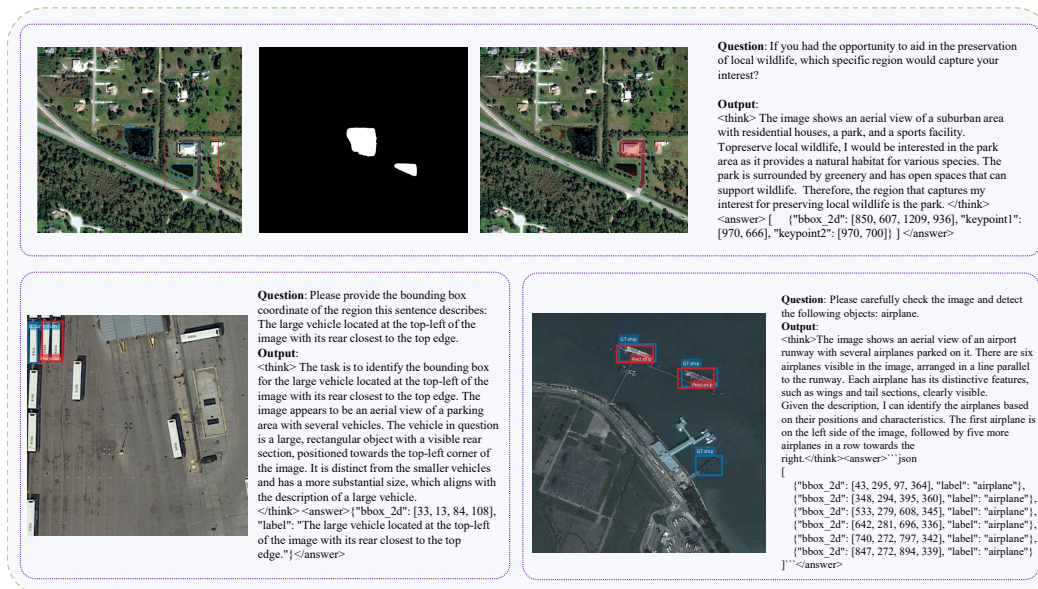


Figure 7: Geo-R1 inference samples (failure case).